Neutron scattering from a collective spin fluctuation mode in a CuO_2 bilayer

N. Bulut and D. J. Scalapino
Department of Physics, University of California, Santa Barbara, California 93106–9530
(Received 21 August 1995)

A resonance in the magnetic scattering of neutrons from superconducting $YBa_2Cu_3O_7$ has been observed at a momentum transfer of $(\pi/a,\pi/a,\pi/\bar{c})$, where a is the in-plane Cu spacing and $\bar{c}$ is the Cu-Cu bilayer spacing. Here we construct a model of a CuO_2 bilayer and show that a collective $S=1$, antiferromagnetic excitation with $\mathbf{q}=(\pi/a,\pi/a,\pi/\bar{c})$ arises if the gap has $d_{x^2-y^2}$ symmetry.

Neutron scattering experiments[1–4] on $YBa_2Cu_3O_7$ find evidence of a narrow resonance in the superconducting state at an energy of 41 meV. Several of these experiments[1,2] also suggest that a weaker broad response appears in the normal state above T_c. In two of these experiments[2,4] polarized neutrons were used to identify the scattering as due to a magnetic excitation, while in another,[3] the momentum dependence of the scattering was used to characterize the magnetic scattering. As a function of momentum transfer, the peak was found to occur at $\mathbf{q}=(\pi/a,\pi/a,\pi/\bar{c})$ with a the in-plane Cu-Cu spacing and $\bar{c}$ the bilayer Cu-Cu spacing.

The challenge in formulating a theoretical framework for interpreting these experiments is that one must deal with both antiferromagnetic and superconducting correlations in a system in which the bilayer band structure and strong Coulomb correlations are important. An approach which we have previously used to discuss NMR (Ref. 5) and neutron scattering[6] involves approximating the magnetic susceptibility χ by a random-phase approximation (RPA) BCS form

$$\chi(\mathbf{q},\omega)=\frac{\chi_0^{\rm BCS}(\mathbf{q},\omega)}{1-\bar{U}\chi_0^{\rm BCS}(\mathbf{q},\omega)}. \tag{1}$$

Here $\bar{U}$ is an effective interaction and

$$\chi_0^{\rm BCS}(\mathbf{q},\omega)=\frac{1}{N}\sum_{\mathbf{p}}\left\{\frac{1}{2}\left[1+\frac{\varepsilon_{\mathbf{p}}\varepsilon_{\mathbf{p+q}}+\Delta_{\mathbf{p}}\Delta_{\mathbf{p+q}}}{E_{\mathbf{p}}E_{\mathbf{p+q}}}\right]\frac{f(E_{\mathbf{p+q}})-f(E_{\mathbf{p}})}{\omega-(E_{\mathbf{p+q}}-E_{\mathbf{p}})+i\delta}\right.$$
$$\left.+\frac{1}{4}\left[1-\frac{\varepsilon_{\mathbf{p}}\varepsilon_{\mathbf{p+q}}+\Delta_{\mathbf{p}}\Delta_{\mathbf{p+q}}}{E_{\mathbf{p}}E_{\mathbf{p+q}}}\right]\frac{1-f(E_{\mathbf{p+q}})-f(E_{\mathbf{p}})}{\omega+(E_{\mathbf{p+q}}+E_{\mathbf{p}})+i\delta}+\frac{1}{4}\left[1-\frac{\varepsilon_{\mathbf{p}}\varepsilon_{\mathbf{p+q}}+\Delta_{\mathbf{p}}\Delta_{\mathbf{p+q}}}{E_{\mathbf{p}}E_{\mathbf{p+q}}}\right]\frac{f(E_{\mathbf{p+q}})+f(E_{\mathbf{p}})-1}{\omega-(E_{\mathbf{p+q}}+E_{\mathbf{p}})+i\delta}\right\} \tag{2}$$

is the BCS susceptibility[7] for a given form of the band structure $\varepsilon_{\mathbf{p}}$ and the gap $\Delta_{\mathbf{p}}$ with $E_{\mathbf{p}}=\sqrt{\varepsilon_{\mathbf{p}}^2+\Delta_{\mathbf{p}}^2}$. Similar approaches to the t-J model have also been used by various authors.[8–11] To model the CuO_2 bilayer in $YBa_2Cu_3O_7$ we have taken

$$\varepsilon_{\mathbf{p}}=-2t(\cos p_x+\cos p_y)-2t_\perp\cos p_z(\cos p_x-\cos p_y)^2-\mu. \tag{3}$$

Here p_x and p_y run over the usual two-dimensional (2D) Brillouin zone and $p_z=0$ or π, corresponding to the bonding or antibonding orbitals of the bilayer. We have assumed a near-neighbor in-plane hopping t and taken an interlayer term of the form suggested in Refs. 12 and 13. For the gap, we will take a simple $d_{x^2-y^2}$ form,

$$\Delta_{\mathbf{p}}=\frac{\Delta_0}{2}(\cos p_x-\cos p_y). \tag{4}$$

Within this approximation, $\chi_0^{\rm BCS}$ treats the pairing correlations while the antiferromagnetic correlations reside in the RPA form for χ, Eq. (1), and the strength of the effective interaction $\bar{U}$. The band structure is contained in $\varepsilon_{\mathbf{p}}$ and the effect of the Coulomb correlations, which reduces the quasiparticle bandwidth and leads to flatbands, will approximately be taken into account by renormalizing t, $t_\perp$, and μ.

Taking $t_\perp/t=0.10$ and $\bar{U}/t=2$, we have calculated $\chi(\mathbf{q},\omega)$ from Eq. (1) for a filling of $\langle n\rangle=0.875$. Results for $\mathrm{Im}\chi(\mathbf{q},\omega)$ versus ω with $\mathbf{q}=\mathbf{Q}=(\pi,\pi,\pi)$ and $\mathbf{q}=\mathbf{Q}'=(\pi,\pi,0)$ in the normal state at $T=T_c$ are shown in Fig. 1(a) as the solid and dashed curves, respectively. Similar results for $\mathrm{Im}\chi(\mathbf{q},\omega)$ versus ω in the superconducting state with $T=T_c/2$ are shown in Fig. 1(b). We have used the same scale in Figs. 1(a) and 1(b) so that the results can be conveniently compared. The resonance in $\mathrm{Im}\chi(\mathbf{Q},\omega)$ occurs for $\omega\simeq\omega_0=2|\mu|$. Here we have taken $T_c=0.1t$ and $\Delta_0(T=0.5T_c)=0.5\omega_0$, corresponding to $2\Delta_0(0)=8kT_c$. We have carried out similar calculations for a dispersion relation with a next-nearest-neighbor hopping term $-4t'\cos p_x\cos p_y$ and found that the peak remains for $\mathbf{Q}=(\pi,\pi,\pi)$ but the structure in $\mathrm{Im}\chi(\mathbf{Q}',\omega)$ for $\mathbf{Q}'=(\pi,\pi,0)$ is further smeared out. The important point is

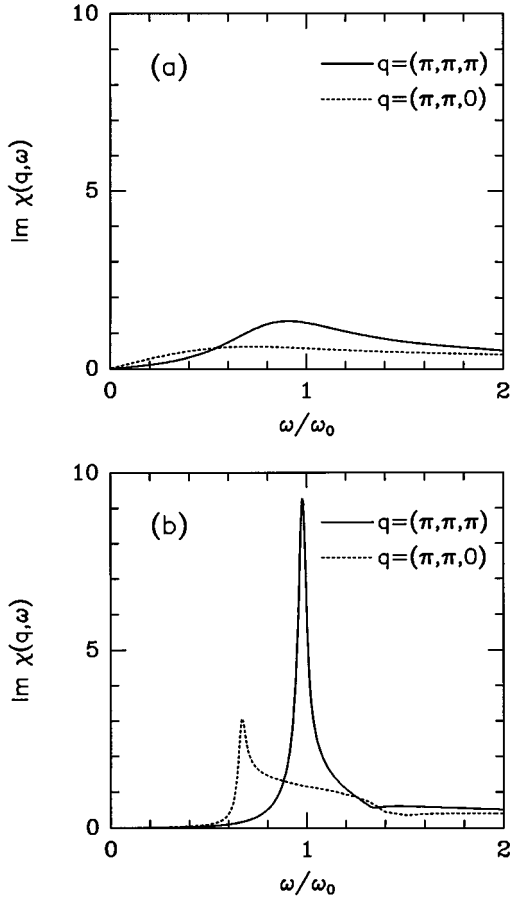

FIG. 1. $\mathrm{Im}\chi(\mathbf{Q},\omega)$ versus ω for $\mathbf{Q}=(\pi,\pi,\pi)$ (solid curve) and $\mathbf{Q}'=(\pi,\pi,0)$ (dotted curve) for (a) the normal state at $T=T_c$ and (b) the superconducting state at $T=T_c/2$. The scales in (a) and (b) are the same for comparison.

that the bilayer coupling makes the nesting of the bonding and the antibonding bands better than the nesting within a given band. Hence, within the RPA framework, the bilayer coupling can cause the peak in $\mathrm{Im}\chi$ to occur at $\mathbf{Q}=(\pi,\pi,\pi)$ rather than at $\mathbf{Q}'=(\pi,\pi,0)$ even for more complicated Fermi surfaces.

In order to understand the origin of the resonance within this model, it is useful to examine the bonding and antibonding energy band contours shown in Fig. 2. The bonding Fermi surface $(\mathbf{p}_F^b,0)$ for $\langle n\rangle=0.875$ is shown as the boundary of the shaded region in Fig. 2(a) and the dotted curve shows the excited bonding energy contour for momentum $(\mathbf{p}_F^b,0)+(\pi,\pi,0)$. Similarly, Fig. 2(b) shows the antibonding Fermi surface and the dotted curve is the excited energy contour for momenta $(\mathbf{p}_F^b,0)+(\pi,\pi,\pi)$. In the normal state, a momentum transfer $\mathbf{Q}=(\pi,\pi,\pi)$ creates a hole on the bonding (antibonding) Fermi surface and scatters a particle to an excited state of the antibonding (bonding) band as illustrated in Fig. 2. For the band structure of Eq. (3), the energy difference

$$\varepsilon_{\mathbf{p}_F+\mathbf{Q}}-\varepsilon_{\mathbf{p}_F}=2|\mu| \tag{5}$$

is independent of $\mathbf{p}_\mathrm{f}$ and one has dynamic nesting[14] which gives rise in the normal state to the broad peak for

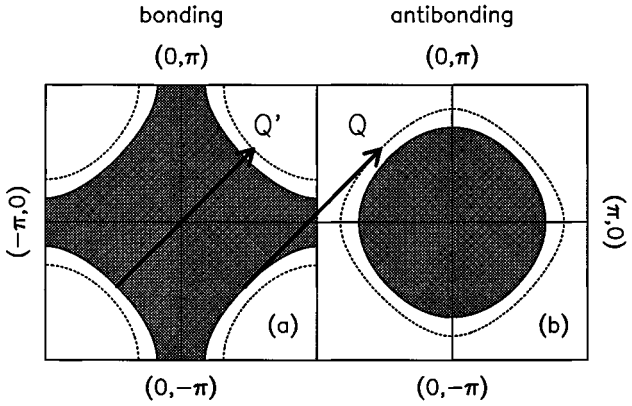

FIG. 2. (a) Bonding (left) and (b) antibonding (right) equal energy contours. The solid lines bounding the shaded regions are the bonding (left) and antibonding (right) Fermi surfaces, respectively. The arrow labeled $\mathbf{Q}$ corresponds to a (π,π,π) momentum transfer which dynamically nests the bonding Fermi surface with an excited antibonding state shown by the dotted curve. Note that a momentum transfer $\mathbf{Q}'=(\pi,\pi,0)$ fails to provide nesting.

$\mathbf{Q}=(\pi,\pi,\pi)$ seen in Fig. 1(a). Here nesting causes $\mathrm{Re}\chi_0$ to increase giving rise to a resonance in $\mathrm{Im}\chi$, Eq. (1). The broadening of this peak is due to the damping associated with $\mathrm{Im}\chi_0$. Depending upon the parameters chosen, the normal state resonance can in fact become more pronounced. The absence of nesting for the intraband transition $\mathbf{Q}'=(\pi,\pi,0)$ in the normal state gives rise to the overdamped dashed curve in Fig. 1(a).

In the superconducting state as a consequence of the $d_{x^2-y^2}$ gap nodes, the interband excitation process shown in Fig. 2 still occurs at $\omega=2|\mu|$ giving rise to a resonance in $\mathrm{Im}\chi(\mathbf{Q},\omega)$ for $\omega\simeq 2|\mu|$. However, in the superconducting state, the broadening of the resonance, determined by $\mathrm{Im}\chi_0(\mathbf{Q},\omega\simeq 2|\mu|)$ is significantly reduced by the opening of the gap as shown in Fig. 3. Furthermore, for a $d_{x^2-y^2}$ gap, $\Delta_{\mathbf{p}+\mathbf{Q}}=-\Delta_{\mathbf{p}}$ and the coherence factor

$$\frac{1}{2}\left(1-\frac{\varepsilon_{\mathbf{p}}\varepsilon_{\mathbf{p}+\mathbf{Q}}+\Delta_{\mathbf{p}}\Delta_{\mathbf{p}+\mathbf{Q}}}{E_{\mathbf{p}}E_{\mathbf{p}+\mathbf{Q}}}\right) \tag{6}$$

which enters the pair production term of Eq. (2) is finite.[6,15] Thus the resonance peak for $\mathbf{Q}=(\pi,\pi,\pi)$ becomes much stronger in the superconducting state as seen in Fig. 1(b). Also as seen in this figure, in the superconducting state a weaker structure can appear in $\mathrm{Im}\chi(\mathbf{Q}',\omega)$ with $\mathbf{Q}'=(\pi,\pi,0)$. However, as noted this structure is further smeared out if next-near-neighbor hopping terms are included in $\varepsilon_{\mathbf{p}}$. In Fig. 4 we have plotted the height of the peak in $\mathrm{Im}\chi(\mathbf{Q},\omega)$ as a function of T/T_c. In our calculation, the intensity of the resonance increases rapidly as the superconducting gap is opened as a consequence of the drop in $\mathrm{Im}\chi_0$ shown in Fig. 3. In calculations of the quasiparticle damping $1/\tau$ due to spin-fluctuation scattering in a $d_{x^2-y^2}$-wave superconductor, it is found that $1/\tau$ drops significantly upon entering the superconducting state.[16] The quasiparticle damping rate obtained from microwave experiments on $YBa_2Cu_3O_7$ also shows a rapid drop in the super-

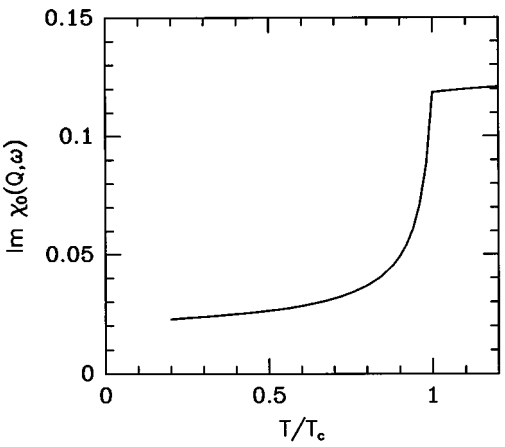

FIG. 3. $\mathrm{Im}\chi_0(\mathbf{Q},\omega)$ versus T/T_c for $\omega \simeq \omega_0$ and $\mathbf{Q}=(\pi,\pi,\pi)$ showing the rapid narrowing of the resonance in the superconducting state. Here we have used the BCS form for the T dependence of Δ_0.

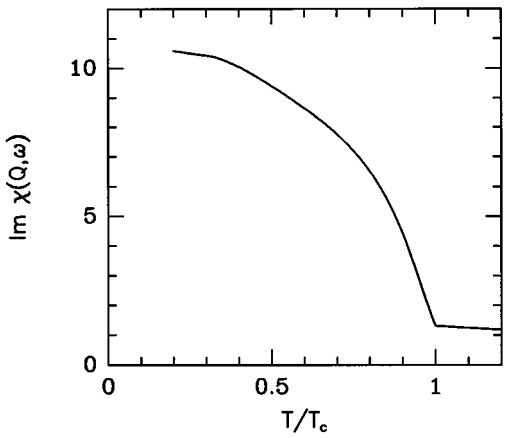

FIG. 4. $\mathrm{Im}\chi(\mathbf{Q},\omega)$ versus T/T_c for $\omega \simeq \omega_0$ and $\mathbf{Q}=(\pi,\pi,\pi)$ showing the growth of the scattering peak in the superconducting state.

conducting state.[17] A sudden drop in the quasiparticle scattering rate can also contribute to the enhancement of the resonance below T_c.

While in this article we have used a particular choice of the band structure, the essential features that we find are more a consequence of the RPA form, Eq. (1), than of the band structure. In fact, one can argue for the existence of a peak at the gap edge of $\mathrm{Im}\chi$ in the superconducting state simply from the RPA form

$$\mathrm{Im}\chi(\mathbf{q},\omega)=\frac{\mathrm{Im}\chi_0(\mathbf{q},\omega)}{[1-U\ \mathrm{Re}\chi_0(\mathbf{q},\omega)]^2+[U\ \mathrm{Im}\chi_0(\mathbf{q},\omega)]^2}. \tag{7}$$

The recent neutron scattering data of Dai *et al.*[4] indicate that within the experimental resolution the spin-fluctuation spectral weight at $\mathbf{Q}=(\pi,\pi,\pi)$ is suppressed for frequencies below that of the resonance upon entering the superconducting state. Within the RPA form, this will imply a suppression of $\mathrm{Im}\chi_0(\mathbf{Q},\omega)$ up to the gap edge, and an enhancement $\mathrm{Re}\chi_0(\mathbf{Q},\omega)$ at the gap edge through the Kramers-Kronig relation. An enhancement of $\mathrm{Re}\chi_0(\mathbf{Q},\omega)$ at the gap edge can cause a resonance in $\mathrm{Im}\chi$ for an antiferromagnetically correlated system. Hence it is possible to interpret the 41 meV peak of the neutron scattering experiments as a particle-hole resonance at the gap edge of an antiferromagnetically correlated $d_{x^2-y^2}$-wave superconductor. The fact that experimentally the resonance occurs at a momentum transfer of (π,π,π) means that within the RPA framework the optimum nesting occurs between the bonding and antibonding bands. Our simple choice of the band structure gives this, as do the local density approximation (LDA) band structure results of Ref. 13.

Thus we conclude that for a $d_{x^2-y^2}$ gap and a bilayer band structure of the type given by Eq. (3) one can understand the occurrence of a resonance in the neutron spin-flip scattering channel at a momentum transfer $\mathbf{Q}=(\pi,\pi,\pi)$ which dramatically narrows and grows in the superconducting state. The energy scale of the resonance implies that $2|\mu|$ is of order 40 meV and the corresponding bandwidth of the quasiparticle dispersion, Eq. (3), used in calculating χ was of order 0.5 eV. We believe that this reduced energy scale arises from the strong Coulomb correlations which renormalize the characteristic quasiparticle energy scale to J and give rise to the flatband behavior seen in angle-resolved photoemission spectroscopy (ARPES) experiments[18,19] and Monte Carlo calculations.[20] It corresponds to the excitation of an antiferromagnetic $S=1$, $\mathbf{Q}=(\pi,\pi,\pi)$ resonance in a bilayer $d_{x^2-y^2}$ superconductor with short range antiferromagnetic correlations. These correlations are allowed by the nodes in the $d_{x^2-y^2}$ gap and persist below T_c just as the transverse NMR T_2^{-1} relaxation rate persists[21,22] below T_c. They reflect a particle-hole resonance which differs from the multiple particle-particle scattering resonance recently proposed by Demler and Zhang.[23]

We thank G. Aeppli, B. Keimer, H. Mook, and S.-C. Zhang for stimulating discussions. The authors gratefully acknowledge support from the National Science Foundation under Grant No. DMR92-25027. The numerical computations reported in this paper were performed at the San Diego Supercomputer Center.

[1] J. Rossat-Mignod, L.P. Regnault, C. Vettier, P. Burlet, J.Y. Henry, and G. Lapertot, Physica (Amsterdam) B **169**, 58 (1991).

[2] H.A. Mook, M. Yethiraj, G. Aeppli, T.E. Mason, and T. Armstrong, Phys. Rev. Lett. **70**, 3490 (1993).

[3] H.F. Fong, B. Keimer, P.W. Anderson, D. Reznik, F. Dogan, and I.A. Aksay (unpublished).

[4] Recent polarized neutron scattering measurements show broad scattering in $\mathbf{q}$ and energy in the normal state that becomes narrow in the superconducting state, resulting in a large feature at 41 meV [P. Dai, H.A. Mook, G. Aeppli, F. Dogan, D. Lee, and K. Salama (unpublished)].

[5] N. Bulut and D.J. Scalapino, Phys. Rev. Lett. **68**, 706 (1992).

[6] N. Bulut and D.J. Scalapino, Phys. Rev. B **47**, 3419 (1993).

[7] J.R. Schrieffer, *Theory of Superconductivity* (Benjamin, Reading, MA, 1964).
[8] H. Fukuyama *et al.*, J. Low Temp. Phys. **95**, 309 (1994).
[9] Q. Si *et al.*, Phys. Rev. B **47**, 9055 (1993).
[10] M. Lavagna and G. Stemmann, Phys. Rev. B **49**, 4235 (1994).
[11] H. Won and K. Maki, Phys. Rev. Lett. **72**, 1758 (1994).
[12] S. Chakravarty, A. Sudbø, P.W. Anderson, and S. Strong, Science **261**, 337 (1993).
[13] O.K. Andersen *et al.*, Phys. Rev. B **49**, 4145 (1994).
[14] Dynamic nesting can also occur for a single layer with $\varepsilon_{\mathbf{p}}=-2t(\cos p_x+\cos p_y)-\mu$.
[15] P. Monthoux and D.J. Scalapino, Phys. Rev. Lett. **72**, 1874 (1994).
[16] S.M. Quinlan, D.J. Scalapino, and N. Bulut, Phys. Rev. B **49**, 1470 (1994).
[17] D.A. Bonn, P. Dosanjh, R. Liang, and W.N. Hardy, Phys. Rev. Lett. **68**, 2390 (1992); D.A. Bonn *et al.*, Phys. Rev. B **47**, 11 314 (1993).
[18] D.S. Dessau *et al.*, Phys. Rev. Lett. **71**, 2781 (1993).
[19] K. Gofron *et al.*, J. Phys. Chem. Solids **54**, 1193 (1993).
[20] N. Bulut, D.J. Scalapino, and S.R. White, Phys. Rev. Lett. **72**, 705 (1994); Phys. Rev. B **50**, 7215 (1994).
[21] N. Bulut and D.J. Scalapino, Phys. Rev. Lett. **67**, 2898 (1991).
[22] Y. Itoh *et al.*, J. Phys. Soc. Jpn. **61**, 1287 (1992).
[23] E. Demler and S.-C. Zhang (unpublished).